









## Article

# Natural Radioactivity in Drinking Water in the Surroundings of a Metamorphic Outcrop in Hungary: The Hydrogeological Answer to Practical Problems

Petra Baják <sup>1,\*</sup>, Bence Molnár <sup>2</sup>, Katalin Hegedűs-Csondor <sup>1</sup>, Mia Tiljander <sup>3</sup>, Viktor Jobbágy <sup>4</sup>, Viktória Kohuth-Ötvös <sup>5</sup>, Bálint Izsák <sup>6</sup>, Márta Vargha <sup>6</sup>, Ákos Horváth <sup>7</sup>, Emese Csipa <sup>8</sup>, Mihály Óvári <sup>8</sup>, Csaba Tóbi <sup>8</sup>, Péter Völgyesi <sup>8</sup>, Krzysztof Pelczar <sup>4</sup>, Mikael Hult <sup>4</sup> and Anita Eröss <sup>1</sup>

<sup>1</sup> József and Erzsébet Tóth Endowed Hydrogeology Chair and Foundation, Department of Geology, Institute of Geography and Earth Sciences, ELTE Eötvös Loránd University, Pázmány Péter sétány 1/C, 1117 Budapest, Hungary; katalin.csondor@tk.elte.hu (K.H.-C.); eross.anita@tk.elte.hu (A.E.)

<sup>2</sup> Department of Geophysics and Space Science, Institute of Geography and Earth Sciences, ELTE Eötvös Loránd University, Pázmány Péter sétány 1/C, 1117 Budapest, Hungary; molbenc@student.elte.hu

<sup>3</sup> Circular Economic Solutions, Geological Survey of Finland, Vuorimiehentie 2K, 02150 Espoo, Finland; mia.tiljander@gtk.fi

<sup>4</sup> European Commission, Joint Research Centre (JRC), Retieseweg 111, 2440 Geel, Belgium; viktor.jobbagy@mail.com (V.J.); krzysztof.pelczar@ec.europa.eu (K.P.); mikael.hult@ec.europa.eu (M.H.)

<sup>5</sup> Sopron Waterwork Ltd., Bartók Béla utca 42, 9400 Sopron, Hungary; kohuth.otvos.viktoria@sopronivizmu.hu

<sup>6</sup> Public Health Laboratory Department, National Public Health Center, Albert Flórián utca 2–6, 1097 Budapest, Hungary; izsak.balint@nnk.gov.hu (B.I.); vargha.marta@nnk.gov.hu (M.V.)

<sup>7</sup> Department of Atomic Physics, Institute of Physics, Eötvös Loránd University, Pázmány Péter sétány 1/A, 1117 Budapest, Hungary; akos@ludens.elte.hu

<sup>8</sup> Nuclear Security Department, Centre for Energy Research, ELKH, Konkoly-Thege Miklós út 29–33, 1121 Budapest, Hungary; csipa.emese@ek-cer.hu (E.C.); ovari.mihaly@ek-cer.hu (M.Ó.); tobi.csaba@ek-cer.hu (C.T.); volgyesi.peter@ek-cer.hu (P.V.)

\* Correspondence: bajakpetra@student.elte.hu



**Citation:** Baják, P.; Molnár, B.; Hegedűs-Csondor, K.; Tiljander, M.; Jobbágy, V.; Kohuth-Ötvös, V.; Izsák, B.; Vargha, M.; Horváth, Á.; Csipa, E.; et al. Natural Radioactivity in Drinking Water in the Surroundings of a Metamorphic Outcrop in Hungary: The Hydrogeological Answer to Practical Problems. *Water* **2023**, *15*, 1637. <https://doi.org/10.3390/w15091637>

Academic Editors: Paolo Fabbri and Dimitrios E. Alexakis

Received: 30 March 2023

Revised: 18 April 2023

Accepted: 20 April 2023

Published: 22 April 2023



**Copyright:** © 2023 by the authors. Licensee MDPI, Basel, Switzerland. This article is an open access article distributed under the terms and conditions of the Creative Commons Attribution (CC BY) license (<https://creativecommons.org/licenses/by/4.0/>).

**Abstract:** Groundwater quality constantly evolves through rock–water interactions, which can enrich groundwater with undesirable elements such as naturally occurring radionuclides. The aim of this study was to understand the cause of gross alpha activity exceeding the screening value of 0.1 Bq L<sup>−1</sup> measured in groundwater-derived drinking water in the vicinity of a metamorphic outcrop in Hungary. As groundwater quality is strongly dependent on the properties of groundwater flow systems, environmental tracers ( $\delta^2\text{H}$  and  $\delta^{18}\text{O}$  composition,  $^{226}\text{Ra}$ ,  $^{222}\text{Rn}$ , total U activity concentration, and  $^{234}\text{U}/^{238}\text{U}$  ratio) and hydraulic evaluation were applied to understand groundwater dynamics. The collected groundwater samples had total U activities up to 540 mBq L<sup>−1</sup>, which translates into an indicative dose below the drinking water parametric value. However, in the presence of dissolved uranium, the  $\delta^2\text{H}$  (−52.6–(−83.4)) and  $\delta^{18}\text{O}$  (−7.17–(−11.96)) values led to the conclusion that local flow systems were sampled that are known to be most vulnerable to any changes in their recharge area. The results confirm that the groundwater flow system approach involving environmental tracers and hydraulic evaluation is a powerful tool for identifying the cause of natural radioactivity in groundwater-derived drinking water.

**Keywords:** drinking water; groundwater flow systems; hydraulic evaluation; uranium; stable isotopes

## 1. Introduction

Groundwater is an essential source of drinking water; however, geogenic contamination can limit its potable use. Understanding the processes that govern groundwater quality is critical for the protection and sustainable management of these resources [1]. Groundwater quality constantly evolves through rock–water interactions during its underground

flow; therefore, understanding flow systems through comprehensive hydrogeological research can be a powerful tool to gain insight into water quality and support drinking water resource management [2,3]. The natural geological and geochemical environment can not only contribute to the composition of groundwater elements that are beneficial for human health (e.g., in the case of mineral water) but can also lead to undesirable or toxic properties due to an excess of certain elements, e.g., naturally occurring radionuclides [4,5]. Groundwater can contain a variety of natural alpha ( $^{234}\text{U}$ ,  $^{238}\text{U}$ ,  $^{232}\text{Th}$ ,  $^{226}\text{Ra}$ ,  $^{222}\text{Rn}$ , and  $^{210}\text{Po}$ ) and beta ( $^{40}\text{K}$ ,  $^{228}\text{Ra}$ , and  $^{210}\text{Pb}$ ) emitters, ranging from undetectable levels to activity concentrations that are a concern to human health [6,7]. The latter is primarily characteristic of areas where the rock framework contains many radioactive elements (e.g., granites, rhyolites, phosphorites, and black shales) [5,8]. Under favourable conditions, primary ore deposits can form in these formations; thus, these areas are generally targeted for fissile material exploration, which includes comprehensive petrographic analysis and geochemical assessment of the rock framework. However, less attention is paid to investigating the radioactive substances that the groundwater may contain. Continuous and organised movement of groundwater can lead to the mobilisation, transport, and accumulation of certain elements, including radionuclides [9,10]. Groundwater flow can modify the primary distribution of radionuclides determined by geological buildup, and secondary radionuclide accumulations can form in rocks relatively distant from the primordial source rock (e.g., sandstone-type uranium deposits) [11,12]. Changing groundwater flow conditions due to climate change and human activity can enhance these processes and remobilise previous accumulations, which may lead to deterioration in the quality of groundwater (i.e., drinking water) [13].

Formations with anomalously high radionuclide content are found near the surface in only a few locations in Hungary. In these areas, the geology favours elevated radionuclide content of the shallow groundwater used for drinking water supply. The Sopron Mountains represent one such location. Most of the Pannonian Basin is covered by young sedimentary rocks, but the crystalline basement outcrop and metamorphic rocks are exposed in this specific area. The Sopron Mountains and their surroundings have a long history regarding natural radioactivity research. In recent years, the area has become the focus of interest since drinking water quality monitoring revealed elevated gross alpha activity ( $>0.1 \text{ Bq L}^{-1}$ ) in waterwork wells drilled in the sedimentary basin situated in the foreland of the mountains. According to the 2013/51/EURATOM Directive, drinking water must also be monitored for radiological parameters [14]. In Hungary, the principles and the procedure of groundwater monitoring, including radioactivity, are contained in the 5/2023 Government Decree, which is currently in force [15]. According to the regulation, besides tritium and radon parameters, gross alpha and gross beta activity measurements must also be used as primary screening methods to assess the risk arising from the radioactive elements in drinking water.

When gross alpha activity exceeds the screening value in the waterwork wells, radionuclide-specific measurements are needed to evaluate whether the effective dose received from drinking water consumption exceeds the  $0.1 \text{ mSv y}^{-1}$  parametric value. For an in-depth understanding of the radioactivity phenomenon, a groundwater flow system approach is a powerful tool, as it explains the systematic distribution of geochemical elements in groundwater [2,16,17].

Consequently, our goal was to apply the flow system theory and its methodology to reveal the cause of elevated gross alpha activity in water wells and to assess the potential health impact. Activity concentrations of the most common alpha emitters in drinking water (i.e.,  $^{234}\text{U}$ ,  $^{238}\text{U}$ ,  $^{226}\text{Ra}$ , and  $^{222}\text{Rn}$ ) were determined, and the interpretation of the results was complemented by hydraulic evaluation and an extensive geochemical evaluation, including measurement of H and O stable isotopic composition and the  $^{234}\text{U}/^{238}\text{U}$  isotopic ratio. This complex approach helps to evaluate the vulnerability of the drinking water supply system and to estimate the effect of human-induced alteration of groundwater flow systems (e.g.,

due to climate change and increasing water demand) on the activity concentrations of naturally occurring radioactive elements in water supply wells [18].

The data presented in this study further expand our knowledge regarding the radioactivity of drinking water in the European Union countries, thereby contributing to the availability of harmonised information and publications about the overall condition of drinking water resources [1,19].

#### *Methods Rationale*

The naturally occurring content of radionuclides in groundwater can be assessed not only in terms of the health effects resulting from their consumption, but they can also be used as environmental tracers to learn about groundwater flow dynamics [20–26]. Therefore, their behaviour in rock–water systems is well-researched [23,24,26–31]. For drinking water quality, the isotopes of uranium, radium, and radon are the most relevant; hence, their properties are briefly discussed below.

The mobilisation of uranium isotopes in groundwater usually occurs in oxidising environments. pH values between 6 and 8 and the high carbonate alkalinity of groundwater further favour their transport [29,32–34]. On the other hand, radium isotopes are mobile under reducing conditions; thus, their presence is especially characteristic of brines with a high dissolved solid content [35–37]. Among the isotopes of radon,  $^{222}\text{Rn}$  has the longest half-life (3.82 days) and is interesting from a hydrogeological point of view.  $^{222}\text{Rn}$  is a noble gas that does not react chemically with either the rock framework or groundwater but is highly soluble in water. Its transport by groundwater is mainly controlled by physical factors (e.g., emanation rate, porosity, permeability, and the presence of structures) [6,38,39], although the adsorption of its mother isotope,  $^{226}\text{Ra}$ , on iron and manganese oxyhydroxides can serve as a local radon source [20,24,40,41].

Due to the significantly distinct geochemical properties of the abovementioned isotopes, their presence is characteristic in different gravity-driven groundwater flow system segments. Oxidative conditions favourable for uranium mobilisation occur in recharge areas or along local flow systems [2,3,16]. On the other hand, radium is expected along intermediate, regional flow paths and in their discharge areas [22–25,41]. Infiltrating water can transport radon in recharge areas, and if there is rapid flow, it can travel greater distances, even to the discharge points of local flow systems [21]. However, its presence is more likely related to radium-rich iron and manganese oxyhydroxide precipitation at the discharge points of regional flow paths [20,24,40,41].

In summary, in presence of each radionuclide, it is possible to draw conclusions about the properties of the groundwater flow system and vice versa; if we know the groundwater flow dynamics, we can estimate which radionuclide will be dissolved in a high activity concentration in the groundwater. The latter can also assist with risk assessment in the drinking water supply.

Measuring not only activity concentration but also isotopic ratios can provide an even more accurate picture of subsurface processes. For instance, examining the natural fractionation of uranium isotopes is an efficient method for identifying isotopically distinct groundwater and geochemical environments [42,43], investigating transport and flow processes in aquifers, and interpreting timescales of weathering [44]. Isotopic fractionation of uranium is usually less significant compared with that of light elements; nevertheless, the  $^{234}\text{U}/^{238}\text{U}$  ratio (AR) has been found to vary considerably (between 0.5 and 40) in groundwater due to natural causes [45,46]. When uranium decays in a closed system,  $^{234}\text{U}$  and  $^{238}\text{U}$  tend to reach a state of secular equilibrium over time, with their ratio settling around 1.0. Under natural circumstances, a deviation from that equilibrium is caused primarily by atomic recoil, leading to the preferential leaching of  $^{234}\text{U}$  compared to  $^{238}\text{U}$  from a solid to solution phase [47,48]. It has to be mentioned that the atomic recoil mechanism is relatively efficient when dissolution rates of the minerals are low and the residence time of groundwater is long [44]. However, AR can also be influenced by other

properties of the system; the age and type of the rocks, climatic effects, and biochemical processes can also affect the variation of  $^{234}\text{U}$  and  $^{238}\text{U}$  isotopes in groundwater [44,48].

Besides radioactive isotopes, stable isotopes of hydrogen and oxygen are also involved. The  $\delta^2\text{H}$  and  $\delta^{18}\text{O}$  composition of water provides supplementary information that is useful to trace groundwater flow. Changes in  $\delta^2\text{H}$  and  $\delta^{18}\text{O}$  can indicate groundwater flow directions, mixtures of different water sources, and rock–water chemical reactions and can identify recharge sources to groundwater [49–52].

The application of different hydrogeochemical and hydrogeological tools supplemented by radioactive and stable isotopic measurements has been effectively used to evaluate groundwater recharge, aquifer heterogeneity, water residence time, and groundwater flow system dynamics, supporting sustainable water resource management and the provision of a safe drinking water supply [52,53].

## 2. Materials and Methods

### 2.1. Study Area

The study area is located in the northwestern corner of Hungary (Figure 1). It encompasses the Hungarian part of the Sopron Mountains and the surrounding lowlands (approx. 363 km<sup>2</sup>). For the maps presented in this study, the Hungarian ‘EOV’ coordinate system (Uniform National Project system) was used. This national coordinate system expresses the easting (as EOV Y) and northing (as EOV X) distances in meters from the system’s origin. The highest point of the study area is located in the Sopron Mountains (577 m above the Baltic Sea level, hereafter referred to as ‘m asl’), while the lowest area is represented by Lake Fertő (ca. 115 m asl). The area has a moderately cool subalpine climate with an increasing average annual temperature (8.5–10 °C) and a decreasing amount of annual precipitation (600–750 mm) towards the east [54–56]. The aridity index varies between 1.06 and 1.10 [56].

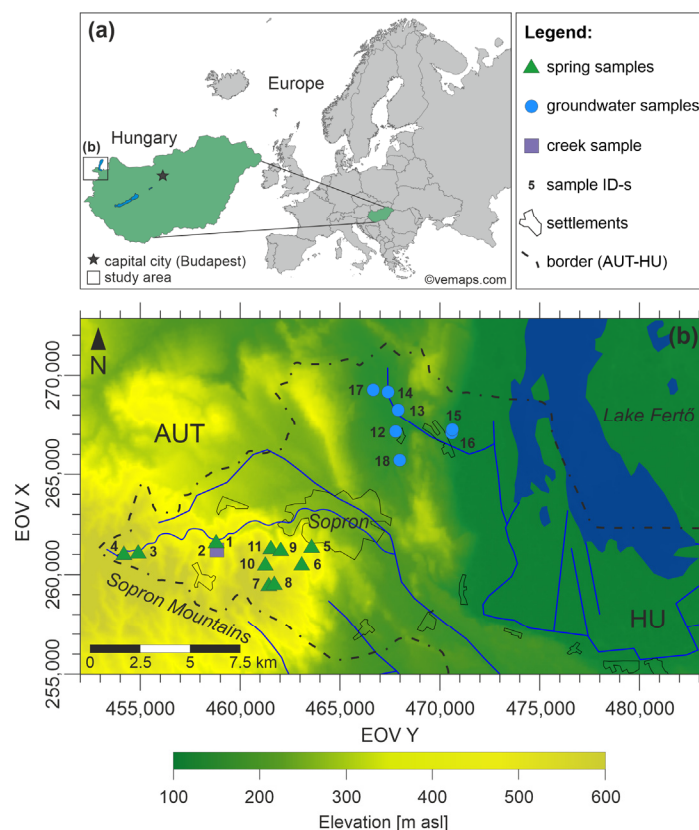


**Figure 1.** (a) The location of the study area. (b) Sampling locations.

Previously, numerous studies investigated the natural radioactivity phenomenon in this area. Between the 1950s and 1970s, the area was surveyed for fissile material [57]. Although no economically productive ore deposits were found, the survey revealed an anomalous uranium concentration (up to  $70 \text{ mg kg}^{-1}$ ) related to specific metamorphic formations (metagranite and leucophyllite) [58]. In addition, secondary uranium enrichment was found to be related to the coaly, clayey formations deposited in the sedimentary basin in the foreland of the Mountains [59]. Research into the natural radioactivity phenomenon has continued ever since. Indoor radon activity was continuously monitored for five years in an artificial gallery of the Geodynamic Observatory of Sopronbánfalva, and extremely high radon activity concentration ( $100\text{--}600 \text{ kBq m}^{-3}$ ) was measured [60]. As for groundwater, springs were also targeted for radon activity measurement, and radon activity up to  $291 \text{ Bq L}^{-1}$  was found [61].

## 2.2. Geological Settings

The study area has a complicated geological build-up (Figure 2). The crystalline basement outcrops in the hilly area are predominantly composed of medium- to large-grade folded orthogneisses and sheared mica schists. Leucophyllites and quartzites appear in subordinate quantities [62–64]. The protoliths of the metamorphic rocks are pelitic sediments and granitic rocks. They suffered a complicated multistage polymetamorphism during which some of the gneisses underwent plastic deformation, resulting in mylonite formation [62,63]. Fluid migration through the mylonites resulted in the precipitation of U-bearing minerals [58,65]. The average U content of  $3.4 \text{ mg kg}^{-1}$  with a maximum of  $70 \text{ mg kg}^{-1}$  was found to be related to the metamorphic formations in the mountains [58,59].

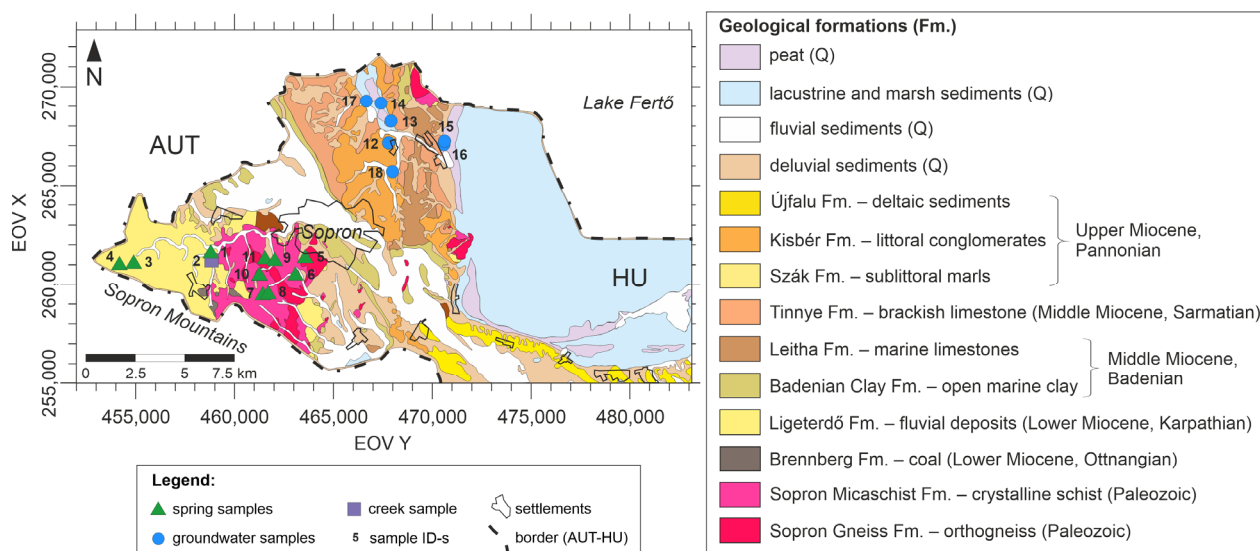


**Figure 2.** Detailed geological map of the study area.

The crystalline basement is unconformably overlain by Miocene and Quaternary sediments. The Miocene sediments, such as sandstone, coal, clay, sandy conglomerate, clayey marl, limestone, and siltstone, were deposited in various depositional settings, including fluvial, marine, and lacustrine environments. The Quaternary sequence includes remnant debris deposited on the slightly steep surface of the metamorphic areas and alluvial, lacustrine sediments along the creeks and by Lake Fertő (clay, gravel, and sand) [66].

## 2.3. Hydrogeological Characterisation

Metamorphic rocks generally have poor hydraulic conductivity ( $10^{-10}\text{--}10^{-13} \text{ m s}^{-1}$ ), but the presence of fractures results in an increase in their conductivity ( $10^{-4}\text{--}10^{-8} \text{ m s}^{-1}$ ) [67]. Due to multiple metamorphic events and recent weathering

processes, the metamorphic rocks in the Sopron Mountains are highly fractured [68]. Numerous springs can be found in the Sopron Mountains that emerge from the weathered and fractured metamorphic rocks or the Miocene to Quaternary siliciclastic sediment cover. Groundwater can penetrate in shallow depths (15–25 m); thus, the springs are characterised by fluctuating discharge rates, low temperature, and low total dissolved solid content [68,69].

In the surroundings of the mountains, the diverse geological setting results in the alternation of aquifer and aquitard layers. The drinking water supply of the region relies exclusively on groundwater resources. Wells are drilled mostly in Miocene Sarmatian formations and screened in conglomerates, sandy–gravely beds, and fractured limestones. Badenian limestone and Pannonian siliciclastic sediments are less significant aquifers in the area. Since these are near-surface aquifers, the average well depth is between 10 and 100 m.

Lake Fertő (Neusiedler See), the largest shallow alkaline lake in Europe, is located in this region, west of the mountains at the Austrian–Hungarian border. The lake has a surface area of 309 km<sup>2</sup> (75 km<sup>2</sup> lies in Hungary), with an average water depth of 1.1 m [70,71]. Due to regulation, the lake's water level varies between 114.5 and 115.5 m asl [72].

#### 2.4. Sampling and Laboratory Measurements

Altogether, 18 water samples were collected for laboratory measurements (Figure 1). The sampling campaign was carried out on 24–25 August 2021. Samples were taken from springs (n = 10), waterwork wells (n = 7), and a creek (n = 1). The springs were included in the study because they bear information about the flow systems as a whole, and they discharge on the metamorphic outcrop in the Sopron Mountains, which is a possible source of radionuclides in the studied region [10,69,73]. The sampled springs are situated between 317 and 465 m asl elevation and emerge from either the metamorphic bedrock or its Miocene and Quaternary sediment cover. Waterwork wells are screened between 18.67 and 91.31 m asl elevation. The wells were selected based on the results of gross alpha measurements. Wells were sampled where gross alpha activity above the 0.1 Bq L<sup>-1</sup> limit was measured (with one exception: sample nr. 18).

The physicochemical properties of the water were recorded on site during each sampling. Specific electrical conductivity (EC) ( $\pm 0.5\%$ ), temperature ( $\pm 0.2$  °C), pH ( $\pm 0.2$ ), oxidation-reduction potential (ORP) ( $\pm 20$  mV), and dissolved O<sub>2</sub> ( $\pm 2\%$ ) were measured by a YSI Pro Plus multiparameter water quality instrument (Xylem, Rye Brook, NY, USA). The accuracy of measurement is provided in parentheses for each parameter. Water samples were collected in 1.5 L PET bottles, 50 mL PP centrifuge tubes, and 0.25 L glass bottles for water chemistry analysis. PP bottles with a capacity of 0.25 L were used to collect samples for total U and <sup>226</sup>Ra measurements. For <sup>222</sup>Rn measurements, 10 mL water samples were taken and injected on site into glass cuvettes previously filled with a 10 mL organic cocktail (Opti-Fluor O, PerkinElmer Inc., Waltham, MA, USA). For the H, O stable isotope measurement, 60 mL water samples were collected in HDPE bottles. In order to preserve the samples, they were refrigerated until the laboratory measurements were performed.

Water chemistry analysis of the samples was performed in the laboratory of the National Public Health Center of Hungary, with one exception: HCO<sub>3</sub><sup>-</sup> concentration was measured in the laboratory of Eötvös Loránd University (ELTE). The concentrations of Na<sup>+</sup>, K<sup>+</sup>, Ca<sup>2+</sup>, and Mg<sup>2+</sup> ions were determined by ICP-MS (iCAP RQ, Thermo Fisher Scientific, Waltham, MA, USA) in accordance with the MSZ EN ISO 17294-2:2017 standard. SO<sub>4</sub><sup>2-</sup>, Cl<sup>-</sup>, and NO<sub>3</sub><sup>-</sup> ion concentrations were measured using ion chromatography (DIONEX ICS-5000 DP, Thermo Fisher Scientific, Waltham, MA, USA) following the MSZ EN ISO 10304-1:2009 standard. For HCO<sub>3</sub><sup>-</sup> measurement, titrimetry was applied (MSZ EN ISO 9963-1:1998 standard).

<sup>222</sup>Rn activity was measured by liquid scintillation detection using a Tricarb 1000 TR device (PerkinElmer, Waltham, MA, USA) at the laboratory of the ELTE Department of Atomic Physics. A cost- and time-effective technique was applied for total U and <sup>226</sup>Ra activity concentration measurements. The so-called NucFilm discs were developed by

Surbeck and can be used for radioactivity measurements of drinking water samples [74]. Two types of discs exist: U-discs are polycarbonate discs coated with epoxy resin, and Ra-discs are polyamide discs stained with MnO<sub>2</sub>. These specific coatings selectively adsorb uranium, polonium, or heavy alkaline earth elements. Only 100 mL of water is required to extract the radionuclides from the water sample. After immersing the Ra disc in the water, the sample is stirred for eight hours to obtain an adsorption efficiency of >90%. As the pretreatment process is completed for <sup>226</sup>Ra measurement, the U-disc is exposed to the exact same water sample after being acidified with 85% formic acid to decrease its pH to between 2 and 3. Acidification ensures the decomposition of uranyl–carbonate complexes. The exposure of the U-disc takes 20 h. After 20 h, 90% of the uranium activity present in the sample is adsorbed.

After extracting the radionuclides from the water sample using chemisorption, the discs are measured by an alpha detector for another 24 h. The expected detection limit using a 100 mL sample for one-day measurement is approximately 5 mBq L<sup>-1</sup> for both total uranium and <sup>226</sup>Ra measurements. Further details on this sample pretreatment and measurement method can be found in the Electronic Supplementary Materials in Baják et al. [75].

The alpha detector in the ELTE Müller-Surbeck laboratory measures the U-discs at ambient pressure. Measurement is easier to perform than in a vacuum and prevents contamination of the detector by recoiled decay products. Due to the absence of vacuum, this method gives the sum of <sup>234</sup>U, <sup>235</sup>U, and <sup>238</sup>U activity concentrations; hence, the term “uranium activity” is used hereafter to refer to the sum of the activity of three uranium isotopes (<sup>234</sup>U + <sup>235</sup>U + <sup>238</sup>U). The <sup>234</sup>U/<sup>238</sup>U isotopic ratio (AR) of the samples was measured in two laboratories because, in the case of drinking water samples, gross alpha activity was also measured to confirm the previous results provided by Sopron Waterwork Ltd., while spring samples were only analysed for AR. Gross measurements could only be performed in one of the laboratories—that of the Joint Research Centre of the European Commission (JRC-Geel). In the JRC-Geel, AR was determined in samples nr. 1, 12, 13, 14, and 17 using a radioanalytical method based on high-resolution alpha-particle spectrometry [76]. The procedure involves preconcentration with iron(III)–hydroxide, coprecipitation, extraction chromatographic separation, and alpha-source preparation using electrodeposition. Samples nr. 2–11, 15, 16, and 18 were analysed for AR in the laboratory of the Centre for Energy Research using a Thermo Element 2 double-focusing ICP-MS instrument (Thermo Finnigan MAT, Bremen, Germany). The following procedure was applied for sample preparation: 10 mL of filtered water sample was acidified with 100 µL cc. HNO<sub>3</sub> was sub-boiled from Suprapur grade (Merck KGaA, Darmstadt, Germany) in single-use PP centrifuge tubes. Then, 4 µg L<sup>-1</sup> of Rh (rhodium) internal standard was added to this solution. Due to high measurement uncertainties, the isotopic ratio could not be determined in samples nr. 6, 7, 8, 10, 11, 15, and 18.

The results of the radioactivity measurements described above are expressed as volumetric activity concentration in mBq L<sup>-1</sup> or Bq L<sup>-1</sup>.

<sup>2</sup>H and <sup>18</sup>O measurements were performed in the isotope laboratory of the Geological Survey of Finland using PICARRO L2130-i <sup>2</sup>H/<sup>18</sup>O an ultra-high-precision isotopic water analyser (Picarro Inc., Santa Clara, CA, USA). The results are normally expressed as δ (‘delta’) values, expressing the isotope ratios of the sample relative to a standard with a known isotopic composition. δ values are calculated according to the following equation and reported per mil (‰) [77]:

$$\delta = [(R_{\text{samples}} - R_{\text{standard}})/R_{\text{standard}}] \times 1000, \quad (1)$$

where  $R_{\text{sample}}$  and  $R_{\text{standard}}$  are the isotope ratios (<sup>18</sup>O/<sup>16</sup>O or <sup>2</sup>H/<sup>1</sup>H) for the sample and the reference material (standard), respectively. Generally, for hydrogen and oxygen, the international VSMOW (Vienna Standard Mean Ocean Water) standard is used [78]. Daily-use in-house standards (calibrated against the VSMOW2-SLAP2 international standards) are utilised to normalise measured δ-values of standards to the VSMOW-SLAP scale. The

uncertainty of the isotopic measurement is <0.1‰ in the case of oxygen analysis and <0.3‰ for hydrogen measurement.

2.5. Hydraulic Evaluation

One approach to investigate the dynamics of the groundwater flow systems is to use the basic regional hydraulic methods of hydrogeology developed by Tóth [10] that are based on his hydraulic continuity theory [73,79]. This methodology uses archive well data, and based on graphical representation, both the horizontal and vertical groundwater flow components can be determined. In Hungary, archive well data are accessible in the data repository of the Supervisory Authority of Regulatory Affairs. In our study area, documentation for a total of 145 wells was processed, which contains all the essential data: (1) well coordinates, (2) elevation, (3) depth of the static water level, and (4) elevation of the screened interval or measuring point (Figure 3a).

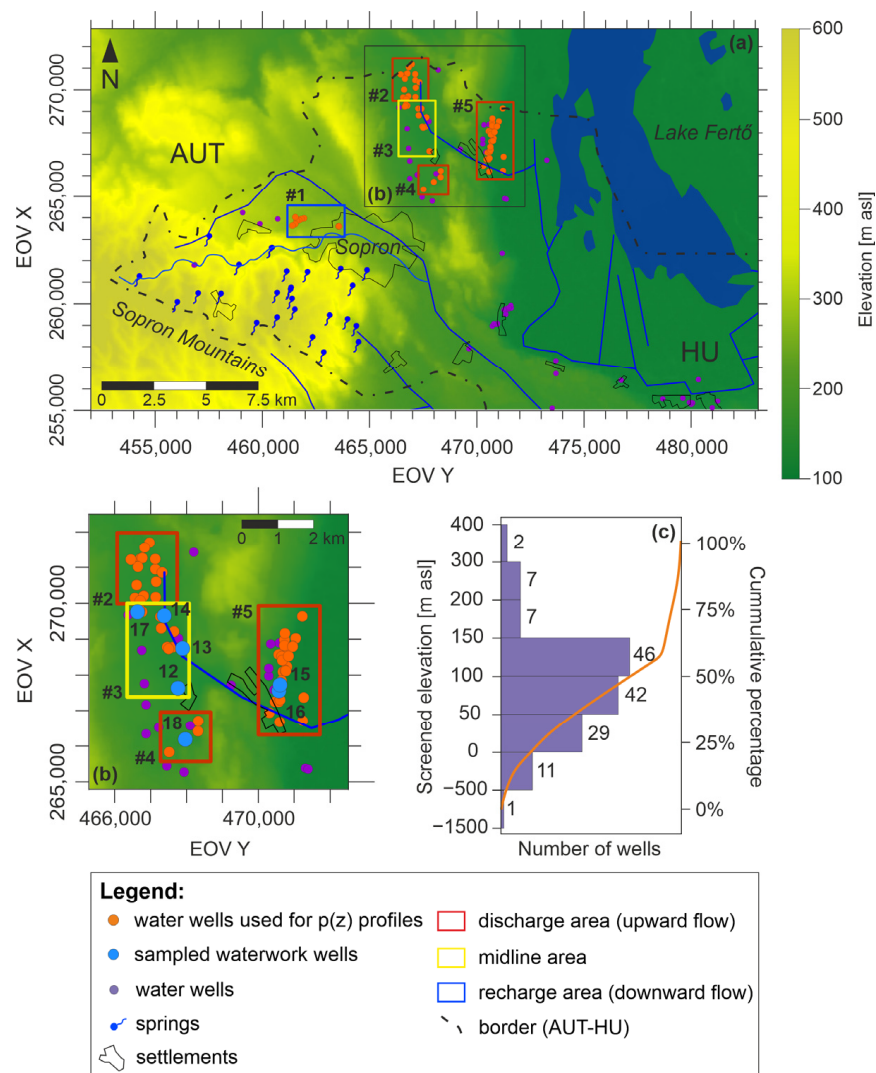


**Figure 3.** (a) Available well data in the study area, the delineated p(z) profile areas, and the related groundwater regime types. (b) The sampled wells are located in p(z) areas nr. 3, 4, and 5. (c) Well data distribution as a function of the screened elevation.

The spatial distribution of the processed wells is sporadic; they are concentrated in the vicinity of small settlements near Lake Fertő. Most of them are screened between 50 and 150 m asl. The Sopron Mountains lack wells, given the metamorphic bedrock, but numerous springs can be found, providing information on the properties of the ground-



water flow systems. As the distribution of wells by geographical location and by depth is poor, compilation of tomographic potential maps for consecutive elevation intervals was not possible based on the collected data (Figure 3c).  $p(z)$  profiles were constructed to understand vertical groundwater flow directions.

By taking into account that (1) wells interpreted in one  $p(z)$  profile should have approximately the same land surface elevation and (2) data points should cover the widest possible depth range and the smallest possible surface area, five  $p(z)$  profiles were made, focusing primarily on the surrounding area of the sampled wells. The following steps were followed to construct  $p(z)$  profiles. First, hydraulic head values were derived using the following calculation: the depth of the static water level (m) was extracted from the wellhead elevation (m asl). Then, the hydraulic head values were converted to pore pressure values using the equation presented below:

$$h = z + p/(\rho \cdot g), \quad (2)$$

where  $h$  is the calculated hydraulic head;  $z$  is the elevation of the measurement point relative to the Baltic Sea level;  $p$  is pore pressure; and  $(\rho \cdot g)$  is the specific weight of the fluid, which is numerically equal to the hydrostatic vertical pressure gradient of that fluid (9.81 MPa km<sup>-1</sup>).

After that, the  $p(z)$  profiles were constructed, plotting the calculated pore pressure values as a function of the elevation of the measurement points. From the regression line equation fitted to the pore pressure values, the vertical pressure gradient can be calculated, indicating the pore pressure change per unit of vertical length. If the system is under hydrostatic conditions, the buoyancy and the force of gravity on the water particles are in balance; thus, there is no vertical fluid flow. In this case, the vertical pressure gradient is called hydrostatic, and its value is  $\gamma_{st} = 9.81 \text{ MPa km}^{-1}$ , assuming a constant water density of 1000 kg m<sup>-3</sup>. When a driving force exists, the system becomes dynamic, and the vertical pressure gradient is also dynamic ( $\gamma_{dyn}$ ). By comparing  $\gamma_{st}$  with  $\gamma_{dyn}$ , the vertical groundwater flow direction can be obtained. Recharge areas are characteristic of  $\gamma_{dyn}$  lower than  $\gamma_{st}$  (subhydrostatic), indicating downward groundwater flow. Discharge areas are characterised by  $\gamma_{dyn}$  higher than  $\gamma_{st}$  (superhydrostatic); therefore, groundwater flow points upward. In midline areas,  $\gamma_{dyn}$  is equal to  $\gamma_{st}$ , meaning that the groundwater flow has no vertical component; however, the horizontal component cannot be excluded. On the  $p(z)$  profiles, the hydrostatic vertical pressure gradient line is also shown to illustrate the difference between  $\gamma_{dyn}$  and  $\gamma_{st}$ .

### 3. Results

#### 3.1. Physicochemical Properties Measured On-Site and Hydrochemistry

Water samples from springs and wells have different characteristics. Table S1 of the Supplementary Materials contains all the measured parameters. Spring waters have low mineralisation (108–697  $\mu\text{S cm}^{-1}$ ), with one exception (sample nr. 1, 1609  $\mu\text{S cm}^{-1}$ ). Creek water has similarly low specific electric conductivity (552  $\mu\text{S cm}^{-1}$ ). Groundwater samples taken from wells have EC values within the range of 708–1198  $\mu\text{S cm}^{-1}$ . Since the total dissolved solids content (TDS) of the water positively correlates with the EC values measured in the water, well water has higher TDS (554–857 mg L<sup>-1</sup>) than spring water (52–482 mg L<sup>-1</sup>) (Figure 4a). Spring sample nr. 1 has remarkably higher TDS than other springs (1115 mg L<sup>-1</sup>), which could be explained by local anthropogenic causes (design of the spring orifice, contamination by tourism, or use of road salt), given its relatively high Cl<sup>-</sup>, SO<sub>4</sub><sup>2-</sup>, K<sup>+</sup>, and Na<sup>+</sup> contents (see Table S1 of the Supplementary Materials).

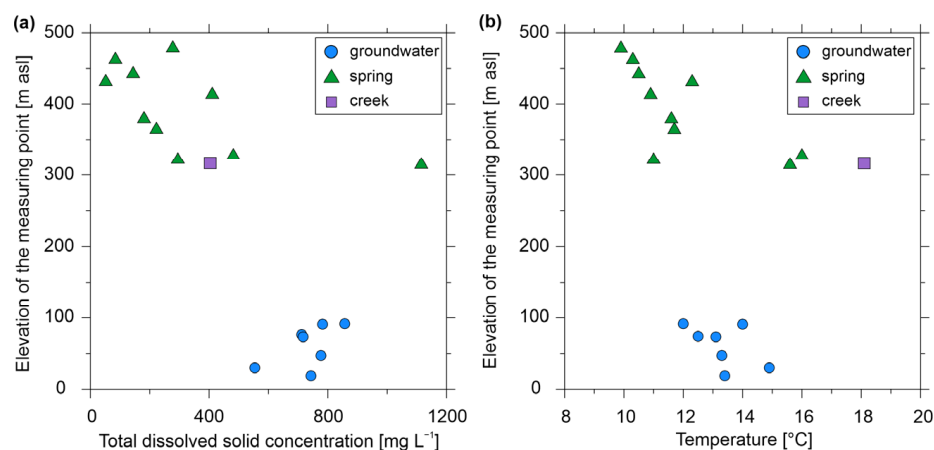


**Figure 4.** (a) Total dissolved solids of the samples as a function of the elevation of the measuring point. (b) Temperature values of the samples as a function of the elevation of the measuring point.

Water samples with different origins cannot be distinguished based on the measured temperature (Figure 4b). The creek sample had the highest temperature of 18.1 °C, but spring and groundwater samples had temperatures between 9.9 and 16.0 °C. The lowest temperature (9.9 °C) was measured in the spring with the highest elevation (481 m asl). Among the spring samples, samples nr. 1 and 5, which are situated in the lowest elevations (317 and 330 m asl, respectively), had the highest temperatures (15.6 and 16.0 °C, respectively). A weak–moderate relationship was found between elevation and temperature (Pearson’s  $R = -0.38$  and related  $P = 0.12$ ; Spearman’s rho,  $r = -0.69$  and related  $p = 0.001$ ), while elevation shows a moderate–strong correlation with TDS ( $R = -0.74$ ,  $P < 0.001$ ,  $r = -0.77$ ,  $p < 0.001$ ) (Figure 4).

The pH of the samples is semineutral (6.14–8.15). Sample nr. 3 has the lowest pH (pH = 6.14), which can be explained by the different origins of the water; according to archive reports, the sampled ‘spring’ could be an outflow from an abandoned borehole drilled in the crystalline basement, probably during fissile material exploration between the 1950s and 1970s [80]. As for the ORP values, positive ORP values were measured in 15 of the 18 samples, indicating the existence of oxidising conditions (42.1–234.1 mV). In the case of the remaining three samples (nr. 12, 13, and 18), negative ORP values were recorded, which may correspond to reducing conditions (−24.6–(−14.9) mV). On-site measurement showed 0.0–4.3 mg L<sup>−1</sup> dissolved oxygen concentration in these latter groundwater samples.

All water samples are characterised by the dominance of an HCO<sub>3</sub><sup>−</sup> anion or no dominant anion (Figure 5). As for cations, there is either no prevalent cation or the sample has Ca dominance. Spring samples have slightly different major ion compositions reflected in their various water types. According to Back [81], the samples were classified into different hydrochemical facies. Samples nr. 1, 6, 10, and 11 belong to the Ca–Na–HCO<sub>3</sub>–Cl–SO<sub>4</sub> facies, similarly to the creek sample (nr. 2). Samples nr. 4, 8, and 9 can be classified as Ca–Na–HCO<sub>3</sub> water type. Sample nr. 5 is of Ca–Mg–HCO<sub>3</sub>–Cl–SO<sub>4</sub> type, and nr. 7 belongs to the Ca–Na–Cl–SO<sub>4</sub>–HCO<sub>3</sub> water type. An outlying sample (nr. 3) has Na–K dominance and can be classified as Na–K–HCO<sub>3</sub>–Cl–SO<sub>4</sub> water type, which is further evidence of the different origin of water compared to the other springs emerging in the Sopron Mountains. Groundwater samples share similar hydrochemical characteristics and can be classified as Ca–Na–HCO<sub>3</sub>–Cl–SO<sub>4</sub> (nr. 12, 15, and 16) and Ca–Mg–HCO<sub>3</sub>–Cl–SO<sub>4</sub> water types (nr. 13, 14, 17, and 18).

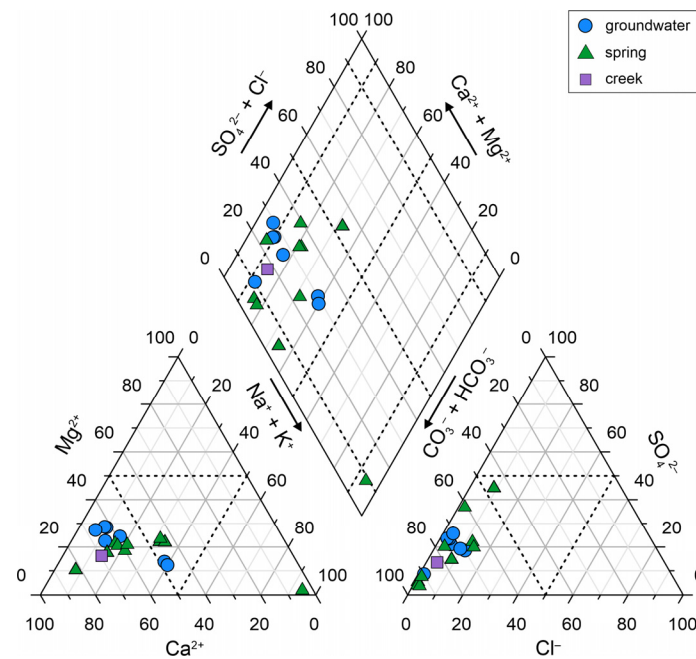


**Figure 5.** Piper diagram showing the common water types based on Back. Arrows indicate increasing concentration [81].

### 3.2. Radionuclide Measurements

Among the analysed radionuclides, total uranium was measured in the highest activity concentration (up to 540 mBq L<sup>-1</sup>) in all sample types (Table S1 of the Supplementary Materials). The highest activities were measured in the groundwater samples (Figure 6). The measured total uranium activities show a moderate correlation with the changes in the elevation ( $R = -0.64, P = 0.004, r = -0.63, p = 0.005$ ). A similar relationship exists between ORP and total uranium activity ( $R = -0.64, P = 0.003, r = -0.57, p = 0.012$ ). These correlations seem reasonable, given that uranium is especially mobile under oxidising conditions, which are present in shallow depth along local flow systems or in recharge areas characterised by downward flow direction.

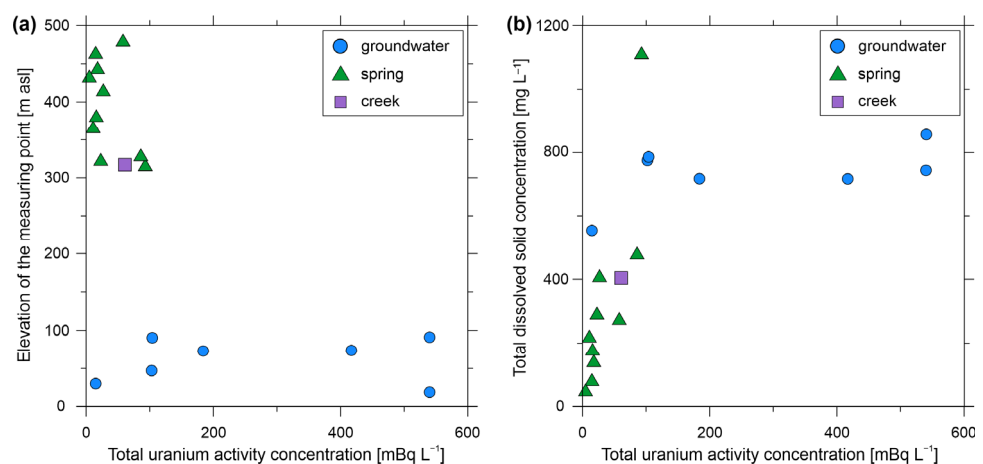


**Figure 6.** (a) Cross plot illustrating total uranium activity concentration (mBq L<sup>-1</sup>) vs. elevation (m asl) of the measuring point. (b) Total uranium activity concentration as a function of the total dissolved solids concentration of the water samples.

Spring waters and the creek had low uranium activity (up to 93 mBq L<sup>-1</sup>). Among spring samples, samples nr. 1 and 5 had the highest activities (86 and 93 mBq L<sup>-1</sup>), as

well as the highest TDS among all spring samples (Figure 6b). Given that these springs are situated at the lowest elevation, these values may be the result of the longer residence time of water compared to the other springs.

$^{226}\text{Ra}$  activity was below or barely above the detection limit of  $5 \text{ mBq L}^{-1}$  in the case of all groundwater, spring, and creek samples (up to  $36 \text{ mBq L}^{-1}$ ).  $^{222}\text{Rn}$  activity of groundwater was measured below the  $100 \text{ Bq L}^{-1}$  drinking water parametric value (up to  $57 \text{ Bq L}^{-1}$ ). On the contrary, spring samples nr. 7 and 8 have  $155.1$  and  $142.9 \text{ Bq L}^{-1}$  activity concentrations, respectively.

Of the analysed samples, only the results of AR measurements in samples nr. 1–5, 9, 12–14, 16, and 17 can be interpreted (Table S3 of the Supplementary Materials). The AR ratios vary between 0.64 and 7.99, indicating a dynamic system in which no radioactive equilibrium exist between the two uranium isotopes [42]. To examine the relationship between  $^{234}\text{U}$  and  $^{238}\text{U}$ , the activity concentration of the isotopes were plotted against each other (Figure 7). The slope of the regression line fitted to the data points represents the AR value. The samples follow two trends: on the one hand, the spring and creek samples have AR values higher than 1.0, the value of AR in secular equilibrium. On the other hand, the AR value measured in groundwater samples is 1.0 or below. Our data gave good correlations, and  $R^2$  calculation shows values of 0.9965 (Trend 1) and 0.9497 (Trend 2).

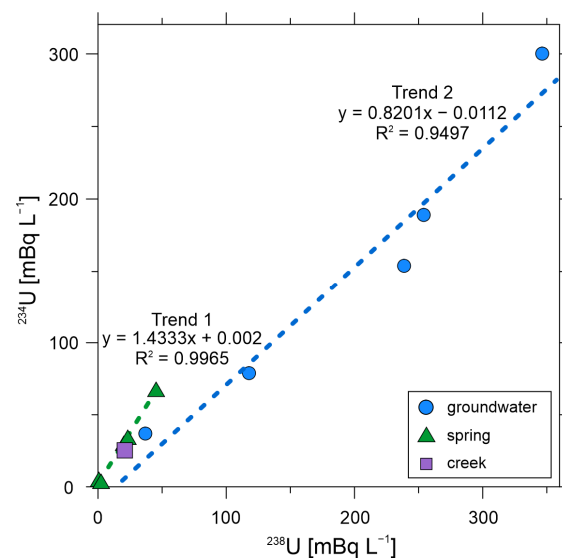


**Figure 7.** Examination of the  $^{234}\text{U}/^{238}\text{U}$  ratio in the analysed water samples.

### 3.3. Stable Isotope Measurements

The stable isotopic composition of water changes continuously within the water cycle. At ambient temperature (i.e., in surface waters and shallow aquifers), the isotopic composition can be considered a conservative property of the water [82]. Therefore, isotopic variations can be applied to characterise the hydrological system within the catchment area or in the aquifer itself [77]. The measured  $\delta^2\text{H}$  and  $\delta^{18}\text{O}$  values are plotted in Figure 8a,b. As groundwater has precipitation origin, we compared our results to the isotopic composition of the global and local precipitation. The  $\delta^2\text{H}$  versus  $\delta^{18}\text{O}$  plot was supplemented with the global meteoric water line (GMWL; [78]) and with a local meteoric water line (LMWL) derived from the stable isotope data of precipitation measured at Farkasfa, a meteorological station in western Hungary [83]. The GMWL and LMWL represent the annual average relationship between  $\delta^2\text{H}$  and  $\delta^{18}\text{O}$  composition of precipitation. LMWL is very similar to GMWL.

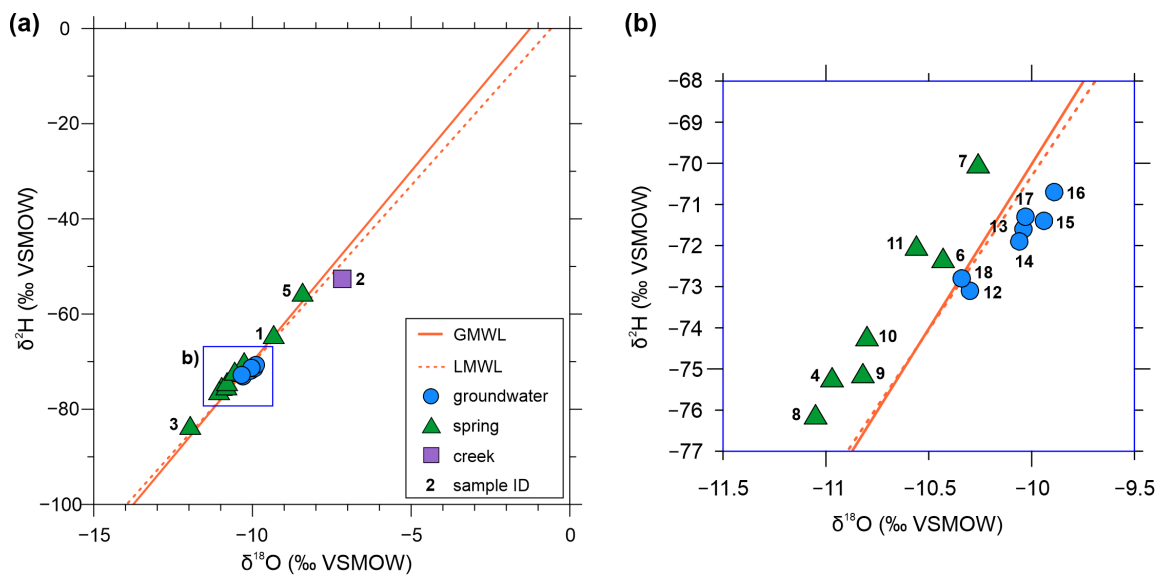


**Figure 8.** (a,b) Stable isotopic composition of the collected water samples. GMWL:  $\delta^2\text{H} = 8 \times \delta^{18}\text{O} + 10$  [78]; LMWL:  $\delta^2\text{H} = 7.48 \times \delta^{18}\text{O} + 4.48$  [83].

Values of  $\delta^{18}\text{O}$  vary from  $-11.96$  to  $-7.17\text{‰}$ , and  $\delta^2\text{H}$  values range between  $-83.4$  and  $-52.6\text{‰}$  (Table S2 of the Supplementary Materials). The samples distributed along the LMWL represent stable isotope values that are characteristic of rainwater under current climatic conditions. The differences in the delta values reflect the annual variation of rainfall and may indicate that spring samples represent rainfall from different altitudes; the springs' orifices are situated between 317 and 481 m asl. The most negative delta values of sample nr. 3 further support the notion that this spring (or abandoned overflowing borehole) is an outlier among the spring samples collected in the mountains, and the delta values may indicate older groundwater recharged under climatic conditions that differ from current conditions [84,85].

Groundwater samples share similar stable isotope characteristics, although the samples can be divided into two groups. Samples nr. 12 and 18 have slightly more negative values than samples nr. 13, 14, 15, 16, and 17, which could be explained by the larger depth of screening of the sampled wells (18.7 and 29.9 m asl) compared to the others (46.9–91.3 m asl). The sample taken from the creek has the least negative delta values among all samples, indicating that the isotopic composition of the creek water is affected by evaporation. This sample also has the lowest d-excess value (4.8, calculated as  $^2\text{H} - 8 \times ^{18}\text{O}$ ). As the spring samples have a similar isotopic composition as the groundwater samples, groundwater, similarly to the springs, has a direct origin from precipitation and a short residence time (i.e., local flow systems).

### 3.4. Hydraulic Evaluation

Given the poor distribution of well data in the hilly part of the study area, five  $p(z)$  profiles could be constructed near the local settlements in the northern part of the study area. Figure 9 summarises the results. The vertical pressure gradient ( $\gamma_{\text{dyn}}$ ) was higher than hydrostatic pressure ( $10.42$ – $11.03 \text{ MPa km}^{-1}$ ), i.e., superhydrostatic in the case of three  $p(z)$  profiles, namely nr. 2, nr. 4, and nr. 5, indicating upward flow in their area.  $\gamma_{\text{dyn}}$  was hydrostatic ( $9.81 \pm 0.5 \text{ MPa km}^{-1}$ ) in the case of  $p(z)$  nr. 3, identifying a midline area. In  $p(z)$  area nr. 1,  $\gamma_{\text{dyn}}$  was lower than hydrostatic ( $8.99 \text{ MPa km}^{-1}$ ), i.e., subhydrostatic, referring to the downward flow direction characteristic in recharge areas. This  $p(z)$  profile has the highest average surface elevation (232.3 m asl), while a lower surface elevation characterises the midline and discharge regime areas.  $p(z)$  nr. 2, 3, and 4 are situated in a local-scale depression called Kõhida Basin with a surface elevation of between 144.9 and

150.9 m asl, while p(z) nr. 5 can be found on the shore of Lake Fertő with the lowest surface elevation of 117.5 m asl among all profiles.

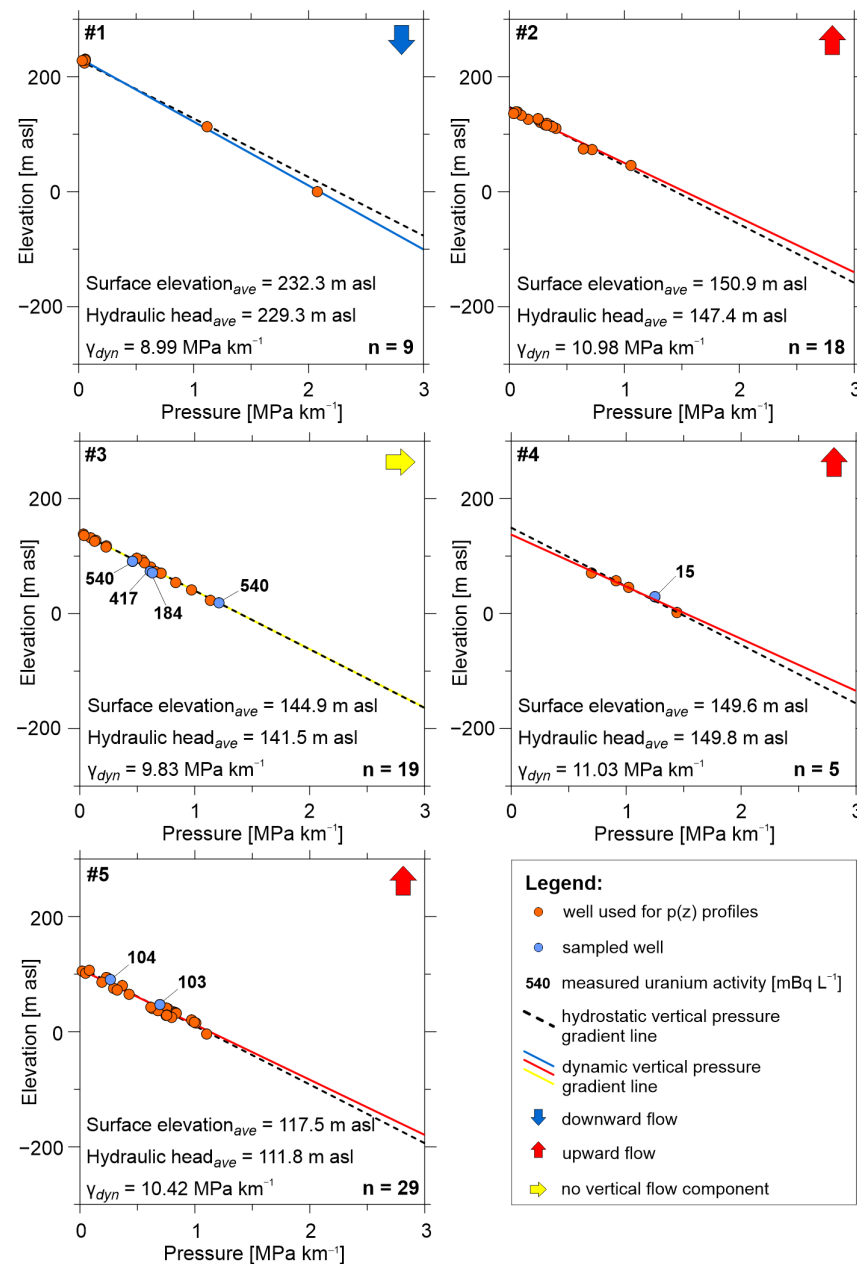


**Figure 9.** Pressure–elevation profiles constructed in the surroundings of the sampled wells. Additionally, total uranium activity concentrations are shown at the elevation of the measurement point of the sampled well. The arrows show the vertical groundwater flow directions.

As for the spatial distribution of the different regime types, the downward flow direction is characteristic in the hilly area, whereas the upward flow direction was identified in the depression of the Kőhida Basin and by Lake Fertő (Figure 3a,b).

#### 4. Discussion

Many springs that discharge in the Sopron Mountains and are characterised by fluctuating discharge rates, low temperature, and low TDS [69,86]. Ten of the numerous springs in the mountains were sampled, and low temperature (9.9–16 °C) and TDS (52–482 mg L<sup>-1</sup>) values were measured. Springs with similar properties can be found

typically at the discharge points of local flow systems [73]. The metamorphic bedrock has low hydraulic conductivity, except for its upper weathered and fractured part. The infiltrated rainwater flows in the regolith at a shallow depth (15–20 m) but discharges a short distance from the infiltration point. The short residence time of water resulted in low TDS and low uranium activity up to  $93 \text{ mBq L}^{-1}$  measured in spring water, as the time is short for rock–water interaction. The direct origin of spring waters from precipitation is also reflected by their stable isotopic composition ( $\delta^2\text{H}$  between  $-55.4$  and  $-83.4$ ,  $\delta^{18}\text{O}$  between  $-8.42$  and  $-11.96$ ), as the sample points are located along the LMWL, indicating recharge from precipitation in today's climate [85,87]. Samples nr. 1 and 5 have the highest uranium activity among all spring samples ( $86$ – $93 \text{ mBq L}^{-1}$ ), which may correspond to a longer residence time of water, given that they are situated near the foot slopes of hills.

Although springs serve as drinking water sources for tourists, the primary drinking water source in the region is the Miocene sediments in the foreground of the Sopron Mountains. Most water wells are screened in shallow depth, between  $50$ – $150 \text{ m}$  asl in sandy–gravely and limestone aquifers. In the collected water samples, low temperatures ( $12$ – $14.9 \text{ }^\circ\text{C}$ ) and TDS ( $554$ – $857 \text{ mg L}^{-1}$ ) were measured, and the dominance of  $\text{Ca}^{2+}$  and  $\text{HCO}_3^-$  characterises the water. These properties indicate the presence of local flow systems in this depth. Like the springs, groundwater samples have stable isotope characteristics referring to direct rainwater origin.

The constructed  $p(z)$  profiles show that the hilly area is a recharge area with a downward flow, while discharge areas characterised by an upward flow can be found by Lake Fertő, in local depressions, and along surface watercourses. Additionally, this picture is influenced by the local variation in topography (variation of hills and depressions), indicating a short residence time between the recharge and discharge points of the groundwater. Based on these findings, the groundwater resources in the foreground of the mountains may not receive recharge from the hilly area because the metamorphic formations have low hydraulic conductivity. The infiltrating water moving in the fractured and weathered part of these metamorphic rocks is discharged in the form of springs. The sedimentary formations in the foreland receive recharge from the nearby local elevations.

Among the radionuclides,  $^{226}\text{Ra}$  was barely above the detection limit (up to  $36 \text{ mBq L}^{-1}$ ).  $^{222}\text{Rn}$  activity above the drinking water parametric value of  $100 \text{ Bq L}^{-1}$  was detected in two springs (samples nr. 7 and 8), but negligible radon activity was measured in the groundwater samples. On the other hand, uranium activity up to  $540 \text{ mBq L}^{-1}$  was measured in the water wells. The lack of dissolved radium and radon and the presence of dissolved uranium can be explained by the dynamics of the groundwater flow system. Positive ORP values were recorded in most samples, referring to an oxidising environment that corresponds well with the presence of local flow systems.

Despite the possibly short residence time of groundwater, the total uranium activity concentration of the groundwater samples was remarkably higher (up to  $540 \text{ mBq L}^{-1}$ ) than in the case of the springs. The source area of the basin-filling sediments was primarily the crystalline rocks in the Sopron Mountains. Uranium transported either by infiltrating water or debris could have accumulated in a favourable environment. According to the outcome of the fissile material survey, syn-sediment enrichment of uranium may be related to the organic matter-rich and clayey sediments in the surroundings of the mountains (Badenian Clay Fm. and Szák Fm.) [59]. Oxygen-rich groundwater can remobilise uranium from these sediments, which causes the elevated total uranium activity concentration of drinking water in this area [88].

From a public health perspective, even the highest activity concentration is one order of magnitude lower than the calculated acceptable level in drinking water ( $3 \text{ Bq L}^{-1}$  for  $^{238}\text{U}$ ,  $2.8 \text{ Bq L}^{-1}$  for  $^{234}\text{U}$ ). The measured uranium activity explains the observed elevated gross alpha activity. However, the derived indicative dose was below the parametric value, so health risk from drinking water consumption is not expected.

Spring and groundwater samples follow two trends based on the AR values measured in the water samples. According to El-Aassy et al. [42], groundwater can be called “normal”

groundwater if the AR is between 1 and 2, while AR values below 1 refer to possible uranium remobilisation. Along with this statement, groundwater samples show signs of remobilisation of uranium, and spring samples are “normal” groundwater samples. The theory of uranium remobilisation is in line with the abovementioned conclusion that uranium accumulated in Miocene sediments is remobilised by the groundwater. Moreover, groundwater with low AR values points to the presence of young water with a more substantial contribution of U due to rock–water interaction and a local recharge component of the groundwater [42], in accordance with the results of  $p(z)$  profiles and the stable isotopes. The significantly high value of AR in sample nr. 3 (7.99) can be explained by rapid change in the geochemical environment [43] or indicate old groundwater [42]. However, since the water’s exact origin is unknown (unidentified borehole), further conclusions cannot be drawn.

## 5. Conclusions

Drinking water quality measures revealed that drinking water of groundwater origin contains radionuclides in the surroundings of the metamorphic outcrop of the Sopron Mountains. Understanding the radioactivity phenomenon has become crucial to understand potential health impacts.

Our results show that both the springs in the mountains and the drinking water resources in the surrounding basin are characterised by low temperature, low TDS, and the dominance of  $\text{Ca}^{2+}$  and  $\text{HCO}_3^-$  ions, which are typical of local flow systems with short residence time and shallow penetration depth, which explains the presence of dissolved uranium in drinking water wells because uranium is mobile under oxidising conditions. However, no health risk arises from the consumption of drinking water (the highest measured uranium activity value is an order of magnitude lower than the derived concentration). As local flow systems are known to be the most sensitive to any changes, climate change and increasing human activity may deteriorate water quality and quantity in the area. Thus, our study identified the high vulnerability of the drinking water resources in the area.

As a methodological conclusion, it can be stated that the Tóthian hydraulic methods, in combination with environmental tracers, are powerful tools for gaining insight into the radioactivity phenomenon and can assist in the risk assessment of drinking water supply systems.

**Supplementary Materials:** The following supporting information can be downloaded at: <https://www.mdpi.com/article/10.3390/w15091637/s1>. Table S1: Physical and chemical properties of the collected water samples; Table S2: Stable isotopic composition of the collected water samples; Table S3:  $^{234}\text{U}/^{238}\text{U}$  ratios measured in the collected water samples.

**Author Contributions:** Conceptualization, P.B., M.V. and A.E.; methodology, P.B., K.H.-C. and A.E.; validation, M.T., V.J., B.I., Á.H., E.C., M.Ó., C.T., K.P. and M.H.; investigation, P.B., B.M., M.T., V.J., B.I., Á.H., E.C., M.Ó., C.T., K.P. and M.H.; resources, M.T., V.J., B.I., Á.H., E.C., M.Ó., C.T., P.V., K.P. and M.H.; data curation, V.J., K.P., E.C., M.Ó. and C.T.; writing—original draft preparation, P.B., K.H.-C. and A.E.; writing—review and editing, M.T., V.J., V.K.-Ö., M.V., M.Ó., P.V., M.H. and A.E.; visualization, P.B.; supervision, V.K.-Ö., M.H. and A.E.; project administration, P.B., B.M., K.H.-C., M.T., V.J. and K.P.; funding acquisition, M.H. and A.E. All authors have read and agreed to the published version of the manuscript.

**Funding:** This topic is part of a project that has received funding from the European Union’s Horizon 2020 Research and Innovation Programme under grant agreement No. 810980. This research was also funded by the National Multidisciplinary Laboratory for Climate Change (RRF-2.3.1-21-2022-00014 project). Furthermore, some radioactivity measurements were supported by the open-access scheme of the European Commission’s Joint Research Centre (JRC) (Research Infrastructure Access Agreement No. 36227-1).

**Data Availability Statement:** The data presented in this study are available upon request from the corresponding author.



**Acknowledgments:** The thorough revisions of the anonymous reviewers and the academic editor are greatly appreciated; their suggestions helped to improve the quality of the paper. The help of László Szikszay in the laboratory and Soma Budai in the fieldwork is gratefully acknowledged. The authors give special thanks the employees of Sopron Waterwork Ltd. who accompanied us during the sampling campaign.

**Conflicts of Interest:** The authors declare no conflict of interest.

## References

- Lapworth, D.J.; Boving, T.B.; Kremer, D.K.; Kebede, S.; Smedley, P.L. Groundwater Quality: Global Threats, Opportunities and Realising the Potential of Groundwater. *Sci. Total Environ.* **2022**, *811*, 152471. [CrossRef] [PubMed]
- Eröss, A.; Csondor, K.; Izsák, B.; Vargha, M.; Horváth, Á.; Pándics, T. Uranium in Groundwater—The Importance of Hydraulic Regime and Groundwater Flow System’s Understanding. *J. Environ. Radioact.* **2018**, *195*, 90–96. [CrossRef] [PubMed]
- Eröss, A. Natürliche Radioaktivität Im Grundwasser—Neue Parameter Und Herausforderungen Für Die Trinkwasserversorgung. *Grundwasser* **2020**, *25*, 111–112. [CrossRef]
- Edmunds, W.M.; Smedley, P.L. Groundwater Geochemistry and Health: An Overview. *Geol. Soc. Lond. Spec. Publ.* **1996**, *113*, 91–105. [CrossRef]
- Vengosh, A.; Coyte, R.M.; Podgorski, J.; Johnson, T.M. A Critical Review on the Occurrence and Distribution of the Uranium- and Thorium-Decay Nuclides and Their Effect on the Quality of Groundwater. *Sci. Total Environ.* **2022**, *808*, 151914. [CrossRef]
- Hoehn, E. Radionuclides in groundwaters: Contaminants and tracers. In *Groundwater Quality: Remediation and Protection*; Herbert, M., Kovar, K., Eds.; IAHS, Publication no. 250; IAHS Press: Wallingford, UK, 1998; pp. 3–9.
- Nuccetelli, C.; Rusconi, R.; Forte, M. Radioactivity in Drinking Water: Regulations, Monitoring Results and Radiation Protection Issues. *Ann. Dell’istituto Super. Sanità* **2012**, *48*, 362–373. [CrossRef]
- Banning, A.; Benfer, M. Drinking Water Uranium and Potential Health Effects in the German Federal State of Bavaria. *Int. J. Environ. Res. Public Health* **2017**, *14*, 927. [CrossRef]
- Skeppström, K.; Olofsson, B. Uranium and Radon in Groundwater—An Overview of the Problem. *Eur. Water* **2007**, *17/18*, 51–62.
- Tóth, J. *Gravitational Systems of Groundwater Flow: Theory, Evaluation, Utilization*; Cambridge University Press: Cambridge, UK, 2009.
- Finch, W.I.; Davis, J.F. *Sandstone-Type Uranium Deposits*; IAEA-TECDOC-328; International Atomic Energy Agency: Vienna, Austria, 1985.
- Grenthe, I.; Drożdżynski, J.; Fujino, T.; Buck, E.C.; Albrecht-Schmitt, T.E.; Wolf, S.F. Uranium. In *The Chemistry of the Actinide and Transactinide Elements*; Springer Netherlands: Dordrecht, The Netherlands, 2018; pp. 253–698.
- Cuthbert, M.O.; Gleeson, T.; Moosdorf, N.; Befus, K.M.; Schneider, A.; Hartmann, J.; Lehner, B. Global Patterns and Dynamics of Climate–Groundwater Interactions. *Nat. Clim. Chang.* **2019**, *9*, 137–141. [CrossRef]
- COUNCIL DIRECTIVE 2013/51/EURATOM. Available online: <https://eur-lex.europa.eu/LexUriServ/LexUriServ.do?uri=OJ:L:2013:296:0012:0021:EN:PDF> (accessed on 14 March 2023).
- 5/2023 Government Decree (in Hungarian: 5/2023 (I. 12) Korm. Rendelet Az Ivóvíz Minőségi Követelményeiről És Az Ellenőrzés Rendjéről). Available online: <https://net.jogtar.hu/jogszabaly?docid=A2300005.KOR&searchUrl=/gyorskereso?keyword%3D5/2023> (accessed on 19 April 2023).
- Baják, P.; Hegedűs-Csondor, K.; Tiljander, M.; Korkka-Niemi, K.; Surbeck, H.; Izsák, B.; Vargha, M.; Horváth, Á.; Pándics, T.; Eröss, A. Integration of a Shallow Soda Lake into the Groundwater Flow System by Using Hydraulic Evaluation and Environmental Tracers. *Water* **2022**, *14*, 951. [CrossRef]
- Csondor, K.; Baják, P.; Surbeck, H.; Izsák, B.; Horváth, Á.; Vargha, M.; Eröss, A. Transient Nature of Riverbank Filtered Drinking Water Supply Systems—A New Challenge of Natural Radioactivity Assessment. *J. Environ. Radioact.* **2020**, *211*, 106072. [CrossRef]
- Ayotte, J.D.; Szabo, Z.; Focazio, M.J.; Eberts, S.M. Effects of Human-Induced Alteration of Groundwater Flow on Concentrations of Naturally-Occurring Trace Elements at Water-Supply Wells. *Appl. Geochem.* **2011**, *26*, 747–762. [CrossRef]
- Gómez, M.; Suursoo, S.; Martin-Sanchez, N.; Vaasma, T.; Leier, M. Natural Radioactivity in European Drinking Water: A Review. *Crit. Rev. Environ. Sci. Technol.* **2023**, *53*, 198–215. [CrossRef]
- Kovács-Bodor, P.; Csondor, K.; Eröss, A.; Szieberth, D.; Freiler-Nagy, Á.; Horváth, Á.; Bihari, Á.; Mádl-Szőnyi, J. Natural Radioactivity of Thermal Springs and Related Precipitates in Gellért Hill Area, Buda Thermal Karst, Hungary. *J. Environ. Radioact.* **2019**, *201*, 32–42. [CrossRef]
- Eisenlohr, L.; Surbeck, H. Radon as a Natural Tracer to Study Transport Processes in a Karst System. An Example in the Swiss Jura. *Comptes Rendus L’academie Sci. Ser. 2 Sci. Terre Planetes* **1995**, *321*, 761–767.
- Eröss, A.; Mádl-Szőnyi, J.; Surbeck, H.; Horváth, Á.; Goldscheider, N.; Csoma, A.É. Radionuclides as Natural Tracers for the Characterization of Fluids in Regional Discharge Areas, Buda Thermal Karst, Hungary. *J. Hydrol.* **2012**, *426–427*, 124–137. [CrossRef]
- Gainon, F.; Surbeck, H.; Zwahlen, F. Natural Radionuclides in Groundwater as Pollutants and as Useful Tracers. In Proceedings of the 12th Symposium on Water Rock Interaction, Kunming, China, 31 July–5 August 2007.

24. Gainon, F.; Goldscheider, N.; Surbeck, H. Conceptual Model for the Origin of High Radon Levels in Spring Waters—The Example of the St. Placidus Spring, Grisons, Swiss Alps. *Swiss J. Geosci.* **2007**, *100*, 251–262. [[CrossRef](#)]
25. Gainon, F. Les Isotopes Radioactifs de LA Série de l'uranium-238 (222Rn, 226Ra, 234U et 238U) Dans Les Eaux Thermales de Suisse: Sites d'Yverdon-Les-Bains, Moiry, Loèche-Les-Bains, Saxon, Val d'Illiez, Bad Ragaz, Delémont, Lavey-Les-Bains, Brigerbad et Combioula. Ph.D. Thesis, Université de Neuchâtel, Neuchâtel, Switzerland, 2008.
26. Swarzenski, P.W. U/Th Series Radionuclides as Coastal Groundwater Tracers. *Chem. Rev.* **2007**, *107*, 663–674. [[CrossRef](#)]
27. Smith, C.G.; Swarzenski, P.W.; Dimova, N.T.; Zhang, J. Natural radium and radon tracers to quantify water exchange and movement in reservoirs. In *Handbook of Environmental Isotope Geochemistry: Volume I*; Springer: Heidelberg, Germany, 2012; pp. 345–365. [[CrossRef](#)]
28. Bourdon, B.; Turner, S.; Henderson, G.M.; Lundstrom, C.C. Introduction to U-Series Geochemistry. *Rev. Miner. Geochem.* **2003**, *52*, 1–21. [[CrossRef](#)]
29. Curtis, G.P.; Davis, J.A.; Naftz, D.L. Simulation of Reactive Transport of Uranium(VI) in Groundwater with Variable Chemical Conditions. *Water Resour. Res.* **2006**, *42*, W04404. [[CrossRef](#)]
30. Grundl, T.; Cape, M. Geochemical Factors Controlling Radium Activity in a Sandstone Aquifer. *Ground Water* **2006**, *44*, 518–527. [[CrossRef](#)] [[PubMed](#)]
31. Cherdynstev, V.V.; Viktor V.; Ivanovich, M.; Harmon, R.S.; Russell S. *Uranium Series Disequilibrium: Applications to Environmental Problems*; Clarendon Press: Oxford, UK, 1982; ISBN 0198544235.
32. Burow, K.R.; Belitz, K.; Dubrovsky, N.M.; Jurgens, B.C. Large Decadal-Scale Changes in Uranium and Bicarbonate in Groundwater of the Irrigated Western U.S. *Sci. Total Environ.* **2017**, *586*, 87–95. [[CrossRef](#)]
33. Coyte, R.M.; Jain, R.C.; Srivastava, S.K.; Sharma, K.C.; Khalil, A.; Ma, L.; Vengosh, A. Large-Scale Uranium Contamination of Groundwater Resources in India. *Environ. Sci. Technol. Lett.* **2018**, *5*, 341–347. [[CrossRef](#)]
34. Alam, M.d.S.; Cheng, T. Uranium Release from Sediment to Groundwater: Influence of Water Chemistry and Insights into Release Mechanisms. *J. Contam. Hydrol.* **2014**, *164*, 72–87. [[CrossRef](#)] [[PubMed](#)]
35. Carvalho, F.; Chambers, D.; Fernandes, S.; Fesenko, S.; Goulet, R.; Howard, B.; Kim, C.-K.; Martin, P.; Moore, W.S.; Phaneuf, M.; et al. *The Environmental Behaviour of Radium: Revised Edition*; International Atomic Energy Agency: Vienna, Austria, 2014.
36. Chałupnik, S.; Wysocka, M.; Janson, E.; Chmielewska, I.; Wiesner, M. Long Term Changes in the Concentration of Radium in Discharge Waters of Coal Mines and Upper Silesian Rivers. *J. Environ. Radioact.* **2017**, *171*, 117–123. [[CrossRef](#)]
37. McMahan, P.B.; Vengosh, A.; Davis, T.A.; Landon, M.K.; Tyne, R.L.; Wright, M.T.; Kulongoski, J.T.; Hunt, A.G.; Barry, P.H.; Kondash, A.J.; et al. Occurrence and Sources of Radium in Groundwater Associated with Oil Fields in the Southern San Joaquin Valley, California. *Environ. Sci. Technol.* **2019**, *53*, 9398–9406. [[CrossRef](#)]
38. Miklyaev, P.S.; Petrova, T.B.; Shchitov, D.V.; Sidiyakin, P.A.; Murzabekov, M.A.; Marennyy, A.M.; Nefedov, N.A.; Sapozhnikov, Y.A. The Results of Long-Term Simultaneous Measurements of Radon Exhalation Rate, Radon Concentrations in Soil Gas and Groundwater in the Fault Zone. *Appl. Radiat. Isot.* **2021**, *167*, 109460. [[CrossRef](#)]
39. Sukanya, S.; Noble, J.; Joseph, S. Factors Controlling the Distribution of Radon (222Rn) in Groundwater of a Tropical Mountainous River Basin in Southwest India. *Chemosphere* **2021**, *263*, 128096. [[CrossRef](#)]
40. Kovács-Bodor, P.; Anda, D.; Jurecska, L.; Óvári, M.; Horváth, Á.; Makk, J.; Post, V.; Müller, I.; Mádl-Szőnyi, J. Integration of In Situ Experiments and Numerical Simulations to Reveal the Physicochemical Circumstances of Organic and Inorganic Precipitation at a Thermal Spring. *Aquat. Geochem.* **2018**, *24*, 231–255. [[CrossRef](#)]
41. Erőss, A.; Surbeck, H.; Csondor, K.; Horváth, Á.; Mádl-Szőnyi, J.; Lénárt, L. Radionuclides in the Waters of the Bükk Region, Hungary. *J. Radioanal. Nucl. Chem.* **2015**, *303*, 2529–2533. [[CrossRef](#)]
42. El-Aassy, I.E.; El-Feky, M.G.; Issa, F.A.; Ibrahim, N.M.; Desouky, O.A.; Khattab, M.R. Uranium and 234U/238U Isotopic Ratios in Some Groundwater Wells at Southwestern Sinai, Egypt. *J. Radioanal. Nucl. Chem.* **2015**, *303*, 357–362. [[CrossRef](#)]
43. Suksi, J.; Rasilainen, K.; Pitkänen, P. Variations in 234U/238U Activity Ratios in Groundwater—A Key to Flow System Characterisation? *Phys. Chem. Earth Parts A/B/C* **2006**, *31*, 556–571. [[CrossRef](#)]
44. Grabowski, P.; Bem, H. Uranium Isotopes as a Tracer of Groundwater Transport Studies. *J. Radioanal. Nucl. Chem.* **2012**, *292*, 1043–1048. [[CrossRef](#)] [[PubMed](#)]
45. Gilkeson, R.; Cowart, J.B. Radium, Radon and Uranium Isotopes in Groundwater from Cambrian-Ordovician Sandstone Aquifers in Illinois. In *Radon in Ground Water*; CRC Press: Boca Raton, FL, USA, 1987; pp. 403–422.
46. Osmond, J.K.; Cowart, J.B. The Theory and Uses of Natural Uranium Isotopic Variations in Hydrology. *Energy Rev.* **1976**, *14*, 621–679.
47. Gascoyne, M. Geochemistry of the Actinides and Their Daughters. In *Uranium-Series Disequilibrium: Applications to Earth, Marine, and Environmental Sciences*; Ivanovich, M., Harmon, R.S., Eds.; Clarendon Press: Oxford, UK, 1992; pp. 34–61.
48. Srivastava, S.K.; Balbudhe, A.Y.; Vishwa Prasad, K.; Padma Savithri, P.; Tripathi, R.M.; Puranik, V.D. Variation in the Uranium Isotopic Ratios 234U/238U, 238U/Total-U and 234U/Total-U in Indian Soil Samples: Application to Environmental Monitoring. *Radioprotection* **2013**, *48*, 231–242. [[CrossRef](#)]
49. Bouchaou, L.; Michelot, J.L.; Vengosh, A.; Hsissou, Y.; Qurtobi, M.; Gaye, C.B.; Bullen, T.D.; Zuppi, G.M. Application of Multiple Isotopic and Geochemical Tracers for Investigation of Recharge, Salinization, and Residence Time of Water in the Souss–Massa Aquifer, Southwest of Morocco. *J. Hydrol.* **2008**, *352*, 267–287. [[CrossRef](#)]

50. Heilweil, V.M.; Solomon, D.K.; Gingerich, S.B.; Verstraeten, I.M. Oxygen, Hydrogen, and Helium Isotopes for Investigating Groundwater Systems of the Cape Verde Islands, West Africa. *Hydrogeol. J.* **2009**, *17*, 1157–1174. [[CrossRef](#)]
51. Negrel, P.; Pauwels, H.; Dewandel, B.; Gandolfi, J.M.; Mascré, C.; Ahmed, S. Understanding Groundwater Systems and Their Functioning through the Study of Stable Water Isotopes in a Hard-Rock Aquifer (Maheshwaram Watershed, India). *J. Hydrol.* **2011**, *397*, 55–70. [[CrossRef](#)]
52. Sun, Z.; Ma, R.; Wang, Y.; Ma, T.; Liu, Y. Using Isotopic, Hydrogeochemical-Tracer and Temperature Data to Characterize Recharge and Flow Paths in a Complex Karst Groundwater Flow System in Northern China. *Hydrogeol. J.* **2016**, *24*, 1393–1412. [[CrossRef](#)]
53. Folch, A.; Menció, A.; Puig, R.; Soler, A.; Mas-Pla, J. Groundwater Development Effects on Different Scale Hydrogeological Systems Using Head, Hydrochemical and Isotopic Data and Implications for Water Resources Management: The Selva Basin (NE Spain). *J. Hydrol.* **2011**, *403*, 83–102. [[CrossRef](#)]
54. Antal, E. A Fertő tó Éghajlata. In *A Fertő tó Természeti Adottságai*; Kovács, Z., Kozmáné Tóth, E., Eds.; Országos Meteorológiai Szolgálat: Budapest, Hungary, 1982; pp. 44–124.
55. Dövényi, Z. *Magyarország Kistájainak Katasztere*, 2nd ed.; Dövényi, Z., Ed.; MTA Földrajztudományi Kutatóintézet: Budapest, Hungary, 2010.
56. Kovács, Z. *Kapuvár Szénhidrogén Koncesszióra Javasolt Terület Komplex Érzékenységi És Terhelhetőségi Vizsgálati Jelentés Tervezete*; Magyar Bányászati és Földtani Szolgálat: Budapest, Hungary, 2019.
57. Földessy, J.; Molnár, F.; Biró, L. Ércföldtan Magyarországon a Földtani Közlöny 150 Évének Tükrében. *Földtani Közlöny* **2020**, *150*, 315–334. [[CrossRef](#)]
58. Török, K. Multiple Fluid Migration Events in the Sopron Gneisses during the Alpine High-Pressure Metamorphism, as Recorded by Bulk-Rock and Mineral Chemistry and Fluid Inclusions. *Neues Jahrb. Mineral. Abh.* **2002**, *177*, 1–36. [[CrossRef](#)]
59. Kósa, L. *A Soproni-Hegység Uránkutatásának Felújítása*; Mecseki Ércbányászati Vállalat: Pécs, Hungary, 1968.
60. Mentés, G.; Eper-Pápai, I. Investigation of Temperature and Barometric Pressure Variation Effects on Radon Concentration in the Sopronbánfalva Geodynamic Observatory, Hungary. *J. Environ. Radioact.* **2015**, *149*, 64–72. [[CrossRef](#)] [[PubMed](#)]
61. Freiler, Á.; Horváth, Á.; Török, K.; Földes, T. Origin of Radon Concentration of Csalóka Spring in the Sopron Mountains (West Hungary). *J. Environ. Radioact.* **2016**, *151*, 174–184. [[CrossRef](#)]
62. Kisházi, P.; Ivancsics, J. A Soproni Gneisz Formáció Genetikai Közettana. *Földtani Közlöny* **1989**, *119*, 153–166.
63. Kisházi, P.; Ivancsics, J. A Soproni Csillámpala Formáció Genetikai Közettana. *Földtani Közlöny* **1987**, *117*, 203–221.
64. Draganits, E. Two Crystalline Series of the Sopron Hills (Burgenland) and Their Correlation to the Lower Austroalpine in Eastern Australia. *Jahrb. Geol. Bundesanst.* **1998**, *141*, 113–146.
65. Török, K. Multiple Fluid Migration Events and REE+Th Mineralisation during Alpine Metamorphism in the Sopron Micaschist from the Eastern-Alps (Sopron Area, Western Hungary). *Földtani Közlöny* **2020**, *150*, 45. [[CrossRef](#)]
66. Haas, J.; Budai, T.; Csontos, L.; Fodor, L.; Konrád, G.; Koroknai, B. Magyarország Prekainozoos Medencealjzatának Földtana Magyarazó “Magyarország Pre-Kainozoos Földtani Térképéhez”; 2014; ISBN 9789636712983. Available online: [https://eles.mbfisz.gov.hu/sites/default/files/file/2018/03/23/aljzat\\_magyarazo.pdf](https://eles.mbfisz.gov.hu/sites/default/files/file/2018/03/23/aljzat_magyarazo.pdf) (accessed on 29 March 2023).
67. Freeze, R.A.; Cherry, J.A. *Groundwater*; Prentice-Hall: Hoboken, NJ, USA, 1979; Volume 39, ISBN 0133653129.
68. Németh, L.; Elsholtz, L. A VI. Számú Kutatócsoport 1959. In *Évi Jelentése a Soproni-Hegység Területén Végzett Radiohidrológiai Kutatásokról*, 1960.
69. Castanea Környezetvédelmi Egyesület. *Sopron Környékének Forrásai*, Sopron, Hungary, 2003.
70. Herzig, A.; Dokulil, M. Neusiedler See—ein Steppensee in Europa. In *Ökologie und Schutz von Seen. Dokulil, M.; Hamm, A., Kohl, J.G., Eds.; Facultas: Wien, Austria, 2001; pp. 401–415.*
71. Löffler, H. *Der Neusiedlersee: Naturgeschichte Eines Steppensees*, 1st ed.; Molden: Graz, Austria, 1974.
72. Magyar, N.; Hatvani, I.G.; Székely, I.K.; Herzig, A.; Dinka, M.; Kovács, J. Application of Multivariate Statistical Methods in Determining Spatial Changes in Water Quality in the Austrian Part of Neusiedler See. *Ecol. Eng.* **2013**, *55*, 82–92. [[CrossRef](#)]
73. Tóth, J. Groundwater discharge: A common generator of diverse geologic and morphologic phenomena. *Int. Assoc. Sci. Hydrol. Bull.* **1971**, *16*, 7–24. [[CrossRef](#)]
74. Surbeck, H. Alpha Spectrometry Sample Preparation Using Selectively Adsorbing Thin Films. *Appl. Radiat. Isot.* **2000**, *53*, 97–100. [[CrossRef](#)] [[PubMed](#)]
75. Baják, P.; Csondor, K.; Pedretti, D.; Muniruzzaman, M.; Surbeck, H.; Izsák, B.; Vargha, M.; Horváth, Á.; Pándics, T.; Erőss, A. Refining the Conceptual Model for Radionuclide Mobility in Groundwater in the Vicinity of a Hungarian Granitic Complex Using Geochemical Modeling. *Appl. Geochem.* **2022**, *137*, 105201. [[CrossRef](#)]
76. Jobbágy, V.; Dirican, A.; Wätjen, U. Radiochemical Characterization of Mineral Waters for a European Interlaboratory Comparison. *Microchem. J.* **2013**, *110*, 675–680. [[CrossRef](#)]
77. Kendall, C.; Caldwell, E.A. Fundamentals of Isotope Geochemistry. In *Isotope Tracers in Catchment Hydrology*; Elsevier: Amsterdam, The Netherlands, 1998; pp. 51–86.
78. Craig, H. Isotopic Variations in Meteoric Waters. *Science* **1961**, *133*, 1702–1703. [[CrossRef](#)]
79. Tóth, J. Hydraulic Continuity In Large Sedimentary Basins. *Hydrogeol. J.* **1995**, *3*, 4–16. [[CrossRef](#)]
80. Jablanczy, S.; Firtás, O. A Soproni Hegyvidéki Erdők Vízirajzi Felvétele. *Az Erdő* **1956**, *5*, 16–20.
81. Back, W. *Hydrochemical Facies and Ground-Water Flow Patterns in Northern Part of Atlantic Coastal Plain*; USGS: Reston, VA, USA, 1966.

82. Gat, J.R. Oxygen and hydrogen isotopes in the hydrologic cycle. *Annu. Rev. Earth Planet. Sci.* **1996**, *24*, 225–262. [[CrossRef](#)]
83. Czuppon, G.; Demény, A.; Leél-Óssy, S.; Óvari, M.; Molnár, M.; Stieber, J.; Kiss, K.; Kármán, K.; Surányi, G.; Haszpra, L. Cave Monitoring in the Béke and Baradla Caves (Northeastern Hungary): Implications for the Conditions for the Formation Cave Carbonates. *Int. J. Speleol.* **2018**, *47*, 13–28. [[CrossRef](#)]
84. Deák, J. Environmental Isotopes and Water Chemical Studies in Hungary for Groundwater Research. In Proceedings of the International Symposium on Isotope Hydrology, Neuherberg, Germany, 19–23 June 1978; IAEA-SM: Neuherberg/Muenchen, Germany, 1978.
85. Fózis, I.; Berecz, T.; Molnár, Z.; Süveges, M. Origin of Shallow Groundwater of Csepel Island (South of Budapest, Hungary, River Danube): Isotopic and Chemical Approach. *Hydrol. Process.* **2005**, *19*, 3299–3312. [[CrossRef](#)]
86. Izápy, G. *Magyarország Forrásainak Katasztere [Natural Spring Cadastral of Hungary]*; OVF-VITUKI Rt. Hidrológiai Intézete: Budapest, Hungary, 2002.
87. Deák, J.; Coplen, T. Identification of Holocene and Pleistocene Groundwaters in Hungary Using Oxygen and Hydrogen Isotopic Ratios. In Proceedings of the Symposium on Isotopes in Water Resources Management, Vienna, Austria, 20–24 March 1995; IAEA: Vienna, Austria, 1996.
88. Pregler, A.; Surbeck, H.; Eikenberg, J.; Werthmüller, S.; Szidat, S.; Türlér, A. Increased Uranium Concentrations in Ground and Surface Waters of the Swiss Plateau: A Result of Uranium Accumulation and Leaching in the Molasse Basin and (Ancient) Wetlands? *J. Environ. Radioact.* **2019**, *208–209*, 106026. [[CrossRef](#)]

**Disclaimer/Publisher’s Note:** The statements, opinions and data contained in all publications are solely those of the individual author(s) and contributor(s) and not of MDPI and/or the editor(s). MDPI and/or the editor(s) disclaim responsibility for any injury to people or property resulting from any ideas, methods, instructions or products referred to in the content.